

An efficient time-stepping scheme for numerical simulation of dendritic crystal growth

Abdullah Shah^a , Muhammad Sabir^a and Peter Bastian^b

^aDepartment of Mathematics, COMSATS Institute of Information Technology, Islamabad, Pakistan;

^bInterdisziplinäres Zentrum für Wissenschaftliches Rechnen, Im Neuenheimer Feld 368, Universität Heidelberg, Germany

ABSTRACT

In this article, we present an adaptive time-stepping technique for numerical simulation of dendritic crystal growth model. The diagonally implicit fractional step θ -scheme for time discretisation and conforming Q_1 finite-element method for space discretisation are used. The performance of the scheme is illustrated by simulating two-dimensional dendritic crystal growth problem, allowing the comparison with other numerical methods. In addition, traditional diagonally implicit Runge–Kutta method is used and comparison is given with the proposed scheme. Robustness is observed for the present scheme. Parametric effects on the growth and shape of dendrites are also given.

ARTICLE HISTORY

Received 11 May 2016
Accepted 21 December 2016

KEYWORDS

Dendritic crystal growth; phase-field model; diagonally implicit fractional step θ -scheme; conforming finite element method

1. Introduction

The numerical simulation of dendritic crystal growth is an essential phenomena in material sciences due to its industrial applications. The growth of such crystals occurs in most alloys and metals (Boettinger et al., 2000), and is closely related to the temperature of the system. In the process of formation of alloys and metals, tiny micro-structures increase in size as a result of solidification and grow with the transformation of the liquid phase into solid phase (Nishinaga & Rudolph, 2014). On the industrial level, the study of shape, size and time scale at which the dendrites are growing is very important due to change in material properties. However, the pattern formation process in dendritic crystal growth is not yet fully understood phenomena (Copley, Todd, Yankova, & Yankov, 1996). Therefore, modelling the complex phenomenon of dendritic crystal growth is very challenging in applied sciences. On one hand, micro-structures are developed in the formation phases that lead to the process of solidification, solid-state precipitation and thermo-mechanical processing. These processes are based on the dynamics of free boundary mechanics and non-equilibrium phase transformation kinetics. In the process of solidification, the

nuclei of grains grow with the consequence to reduce the surface free energy of the system due to diffusion of mass and heat. On the other hand, the driving forces that lead to thermodynamics are variable. Freezing or solidification generally serves as a model with many modes of non-equilibrium phase transition underlying complex micro-structure formation. The pattern formation is well known because it solidifies at room temperature and allows one to look at how solidification process takes place. However, materials that are rich in dendrites are more likely to be corrosive and hence vulnerable (Fix, 1983). The idea to simulate two-phase flow problems with jump discontinuities at sharp interface was first given by Fix Wang and Sekerka (1993). From mathematical point of view, such problems are called moving boundary problem where the interface has varying behaviours due to different material properties of the two phases. However, problems with sharp interface are difficult to solve analytically or numerically. An alternative of sharp interface model like level set method (Osher & Sethian, 1988) is the phase-field model where the sharp interface is replaced by diffusive region of small thickness. The basic idea of phase-field model is to introduce an order parameter that varies continuously over thin interfacial region and is mostly uniform in the bulk phases. In recent years, this idea became very popular in computational material sciences, solid-state physics and multi-phase flows due to inherited simplicity at the interface. The phase-field model having coupled system of parabolic partial differential equations (PDE's) was first used by Levine et al. Collins and Levine (1985) and Kobayashi (2006) to simulate the dendrite growth phenomena of solidification under-cooling. Further, an extensive effort is made by Jimack's et al. Bollada, Jimack, and Mullis (2012), Goodyer, Jimack, Mullis, Dong, and Xie (2012), Mullis, Bollada, and Jimack (2014), Mullis, Goodyer, and Jimack (2012), in developing numerical techniques for solidification with focus on mesh size, its refinement and de-refinement. In view of his work including others, it is still a desire to develop efficient time discretisation scheme which allows the simulation of solidification process for large time-step to reduce the computing cost.

Stiff PDEs arises in modelling many physical systems where two or more different processes are combined. Numerical methods for solving such PDEs need more work per time-step. Explicit methods are conditionally stable for such problems, while the implicit methods are more numerically stable with larger step size. Alexander (1977) solved stiff problems using diagonally implicit Runge–Kutta (DIRK) methods of different orders of accuracy. The main aim of this paper is to provide an efficient and accurate numerical scheme for simulating dendritic growth type of stiff problem using the PDELab (Bastian, Blatt, Dedner, Engwer, Kl'ofkorn, Kornhuber, Ohlberger et al., 2008; Bastian, Blatt, Dedner, Engwer, Kl'ofkorn, Kornhuber et al., 2008; Blatt & Bastian, 2007, 2008; Dedner, Kl'ofkorn, Nolte, & Ohlberger, 2010). The PDELab is a discretisation module based on Distributed and Unified Numerics Environment (DUNE) (Bastian et al., 2006), which is an open source software. The PDELab is rapid

prototyping which substantially reduce time to implement discretisation and solver for system of PDEs. It is successfully used for numerical solution of many elliptic, parabolic and hyperbolic PDEs arising from different application areas (Bastian & Helmig, 1999; Bastian & Rivière, 2004). In PDELab, different discretisation schemes like conforming finite element, discontinuous Galerkin finite element and cell-centred finite volume method are used. It also includes multi-grid approach for solving linear and nonlinear system of PDEs with special emphasis on computational efficiency and accuracy.

The rest of the paper is organised as follows. Section 2 gives the governing equations for the dendritic crystal growth due to thermal diffusion. Section 3 describes space and time discretisation schemes. Solution to a test problem to check the adaptivity factor of traditional DIRK scheme (Alexander, 1977) and comparison with proposed diagonally implicit fractional step θ (DIFST) scheme are given in Section 4. Parametric effects on the growth and shape of dendrites are given in Section 5. Section 6 concludes this paper.

2. Governing equations

The phase-field method is a mathematical technique for a two-phase flow in which the sharp interface between both phases is replaced by the non-zero transition layer (Wheeler, Murray, & Schaefer, 1993) of thickness ϵ and introducing a phase function $c(\mathbf{x}, t)$ whose value varies from 0 to 1. For example, it is '0' in liquid phase and '1' in the solid phase and the intermediate value between 0 and 1 refers to the phase transition region (Biben, 2005) containing the interface. The mathematical model of solidification is a coupled system of two parabolic PDEs; one for ' $c(\mathbf{x}, t)$ ' which propagates phase function and the other for thermal diffusion which comprises the dimensionless temperature $T(\mathbf{x}, t)$. The governing equations can be written as follows Biben (2005), Wheeler et al. (1993), Shah, Haider, and Shah (2014):

$$\tau \frac{\partial c}{\partial t} = -\frac{\delta G(c)}{\delta c}, \quad (1)$$

$$\frac{\partial T}{\partial t} = \nabla^2 T + k \frac{\partial c}{\partial t}. \quad (2)$$

The term $\frac{\delta G(c)}{\delta c}$ is the functional (variational) derivative of the square-gradient free energy functional $G(c)$. $G(c)$ measures the energy in the interface and describes the solid and liquid phases. The total energy of the transition layer decreases by minimisation of gradient free energy functional due to negative sign in Equation (1) and the term δ signifies the functional (variational) derivative operator. The square-gradient free energy functional is given by McFadden, Wheeler, Braun, Coriell, and Sekerkan (1993):

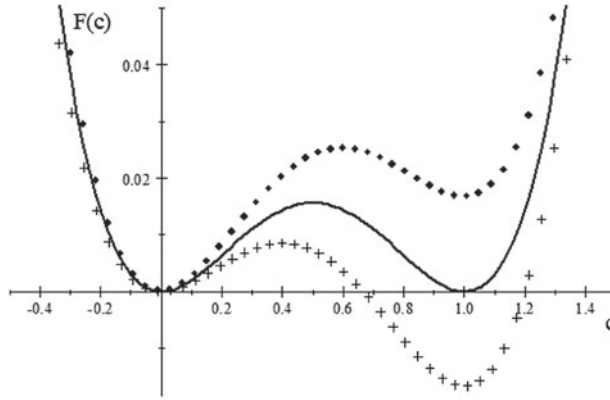


Figure 1. Schematic view of the double well potential free-energy functional: dotted line ($n < 0$), solid line ($n = 0$) and crossed line ($n > 0$).

$$G(c) = \int \left[F(c) + \frac{\epsilon^2 (\nabla c)^2}{2} \right] dx,$$

where

$$F(c) = \frac{1}{4}c^4 - \left(\frac{1}{2} - \frac{n}{3}\right)c^3 + \left(\frac{1}{4} - \frac{n}{2}\right)c^2 \quad (3)$$

is the double well free energy functional which accounts for the growth of solid phase at the expense of liquid phase. The coefficient in Equation (3) is simply chosen to force the two minima to be 0 and 1. The parameter n gives a thermodynamical driving force which leads to the growth of solid phase due to the difference of actual temperature T and melting temperature T_m . One can adopt several prescriptions for n to fix the distance to equilibrium. However, we choose the Kobayashi's prescription $n(T) = \frac{\beta}{\pi} \tan^{-1} [\eta (T_m - T)]$ given in reference (Kobayashi, 2006), where β and η are positive constants. By taking $\beta < 1$ ensures $|n(T)| < \frac{1}{2}$ for all values of T . From Figure 1, we can see that $n > 0$ leads to the solid phase ($c = 1$) whereas $n < 0$ leads to the liquid phase ($c = 0$) and $n = 0$ is the phase equilibrium. The difference of two minimum values is proportional to n (i.e. $F(0) - F(1) = n/6$), which gives a difference of chemical potential of the both phases.

In the numerical description of dendrites growth, the anisotropy which exists on the solid/liquid interface must be considered. To take anisotropy into account, Kobayashi assumed an angular dependence of the interfacial width $\epsilon = \epsilon(\phi) = \epsilon_0 (1 + \mu \cos(a_0(\phi - \phi_0)))$, where ϕ_0 , a_0 and μ are the orientation of the anisotropy axis, the modulation of interface and anisotropic mode number, respectively. The anisotropic mode number a_0 gives the main branches of the dendrites. Since the thermodynamical driving forces enter the dendrite growth problem through the Gibbs–Thomson condition, which relates the local equilibrium temperature to the interface curvature. In multi-dimensions, interface curvature is a scalar quantity $\epsilon = \epsilon(\phi)$, where ϕ is the angle between ∇c and

a fixed reference axis. For the positive value of μ , interface curvature minima correspond to x -axis dendrite growth directions (Haxhimali, Karma, Gonzales, & Rappaz, 2006; McFadden et al., 1993). The growth of solid phase is due to thermal gradient in which the solid-liquid interface melts and reduces to the angle ϕ .

Equation (2) is the heat equation with a source term $k \frac{\partial c}{\partial t}$ that maintains the energy difference in both phases. The source term also ensure the limitation for effect of liberation of latent heat coefficient k at the interface. The two-dimensional form of the Equations (1)–(2) can be extended as McFadden et al. (1993);

$$\tau \frac{\partial c}{\partial t} = \nabla \cdot ((\epsilon^2 \mathbf{I} + \epsilon \epsilon' \mathbf{A}) \nabla c) + c(1-c)(c-0.5+n), \quad (4)$$

$$\frac{\partial T}{\partial t} = \nabla^2 T + k \frac{\partial c}{\partial t}, \quad (5)$$

$$\text{with } \mathbf{I} = \begin{bmatrix} 1 & 0 \\ 0 & 1 \end{bmatrix} \text{ and } \mathbf{A} = \begin{bmatrix} 0 & -1 \\ 1 & 0 \end{bmatrix},$$

where $\epsilon' = \frac{d\epsilon}{d\phi}$. Solution of Equation (4) describes the shape, motion and location of the interface, while the solution of Equation (5) describes the temperature variation. The system is subject to initial conditions $c(\mathbf{x}, 0) = c_0$ and $T(\mathbf{x}, 0) = 0$ while no-flux condition is imposed on the boundaries.

3. Numerical discretisation

Finding the analytical solution of Equations (4)–(5) is not easy. However, an approximate numerical solution can be computed using appropriate numerical method. For this purpose, we adapted the Q_1 conforming finite-element method (FEM) (Glowinski, 2003; Hughes, 2008; Madzvamuse, 2006; Thomee, 2006) for spatial discretisation along with proposed DIFST scheme for temporal discretisation. The main advantage of the DIFST scheme is that it treats non-linear terms implicitly (Ruuth, 1995). The efficiency of the scheme is demonstrated by comparing it with DIRK2 and DIRK3 schemes. The detail of discretisation schemes is as follow.

3.1. Spatial discretisation

In the FEM, the weak formulation can be obtained by multiplying Equations (4)–(5) with appropriate test functions u and v , respectively, and using integration in space by parts to evaluate the integrals. The main advantage of FEM is to easily treat the full tensor and its flexibility in calculating mass and stiffness matrices analytically using global basis functions directly.

We find $(c, T) \in X$ such that:

$$\int_{\Omega} \left(\tau \frac{\partial c}{\partial t} u \right) dx + \int_{\Omega} ((\epsilon^2 \mathbf{I} + \epsilon \epsilon' \mathbf{R}) \nabla c \cdot \nabla u) dx - \int_{\Omega} (f(c) u) dx = 0, \quad u(0) = 0 \quad (6)$$

$$\int_{\Omega} \left(\left(\frac{\partial T}{\partial t} - k \frac{\partial c}{\partial t} \right) v \right) dx + \int_{\Omega} (\nabla T \cdot \nabla v) dx = 0, \quad v(0) = 0, \quad (7)$$

$\forall u, v \in Y$, where X is the space of trial functions and Y is the space of test functions. The formulation (6)–(7), is weaker than (4)–(5) as it imposes the weaker conditions on smoothness of solution (c, T) and test functions (u, v) . In fact

$$X = \left\{ w = w(x, y) : w, \frac{\partial w}{\partial x}, \frac{\partial w}{\partial y} \in L^2(\Omega), w = 0 \text{ on } \partial\Omega \right\}$$

and, in this case, $X = Y$. The space X is usually denoted by

$$X = \{ w \in H^1(\Omega), w = 0 \text{ on } \partial\Omega \}$$

where $H^1(\Omega)$ is the Sobolev space of functions on Ω with generalised derivatives $L^2(\Omega)$. Since only the first-order derivative of c and T is involved in Equations (6)–(7), so method of line is suitable to solve the system. For this purpose, we used Q_1 conforming FEM. The main task is to approximate the solutions $c(\mathbf{x}; t)$ and $T(\mathbf{x}; t)$ by finite element solutions $c_h(\mathbf{x}; t)$ and $T_h(\mathbf{x}; t)$, respectively (h being the mesh size) i.e.

$$c(\mathbf{x}; t) \approx c_h(\mathbf{x}; t) = \sum_{j=1}^N U_j(t) \Phi_j(\mathbf{x}), \quad (8)$$

$$T(\mathbf{x}; t) \approx T_h(\mathbf{x}; t) = \sum_{j=1}^N V_j(t) \Psi_j(\mathbf{x}). \quad (9)$$

By substituting Equations (8)–(9) into Equations (6)–(7), respectively, we get the following system of ordinary differential equations,

$$\mathbf{M} \frac{d\mathbf{U}}{dt} + \mathbf{K}\mathbf{U} - \hat{\mathbf{F}} = 0, \quad (10)$$

$$\mathbf{N} \frac{d\mathbf{V}}{dt} - \mathbf{P} \frac{d\mathbf{U}}{dt} + \mathbf{G}\mathbf{V} = 0, \quad (11)$$

for the vectors of coefficient functions $\mathbf{U} = U_j(t)$ and $\mathbf{V} = V_j(t)$ for $j = 1, 2, 3 \dots N$. $\mathbf{M} \in \mathbb{R}^N \times \mathbb{R}^N$, $\mathbf{N} \in \mathbb{R}^N \times \mathbb{R}^N$ and $\mathbf{P} \in \mathbb{R}^N \times \mathbb{R}^N$ are mass matrices, $\mathbf{K} \in \mathbb{R}^N \times \mathbb{R}^N$, $\mathbf{G} \in \mathbb{R}^N \times \mathbb{R}^N$ are stiffness matrices and $\hat{\mathbf{F}} \in \mathbb{R}^N$ is a vector for non-linear terms known as load vector.

Table 1. Comparison of different time discretization schemes for $\sigma = 1.1$.

$\sigma = 1.1$	TIME STEPS	MAX L-IT	MAX NL-IT	CPU TIME	LS TIME
DIFST	79	1213	538	2474.7	086.07
DIRK3	79	3370	603	2903.9	259.58
DIRK2	Fails after 46 time steps with $\Delta t > 8.7017 \times 10^{-4}$				

3.2. Temporal discretisation

Due to continuity with respect to time and non-linearity of the matrix, \hat{F} does not permit us to find the solution in a straightforward way. Also to avoid time-step restriction, it is intended to apply an implicit or diagonally implicit time-stepping scheme. For this purpose, we modified the implicit fractional-step θ -scheme (Madzvamuse, 2006) in the fashion of DIRK scheme into second-order three-stage DIFST scheme given as follows:

In first stage, solve the pair $(\mathbf{U}^{n+\theta}, \mathbf{V}^{n+\theta})$ as:

$$\begin{aligned} \mathbf{M} \frac{\mathbf{U}^{n+\theta} - \mathbf{U}^n}{\theta \Delta t} + \alpha K \mathbf{U}^{n+\theta} + (1 - \alpha) K \mathbf{U}^n - \alpha \hat{F}(\mathbf{U}^{n+\theta}) - (1 - \alpha) \hat{F}(\mathbf{U}^n) &= 0, \\ \mathbf{N} \frac{\mathbf{V}^{n+\theta} - \mathbf{V}^n}{\theta \Delta t} - \mathbf{P} \frac{\mathbf{U}^{n+\theta} - \mathbf{U}^n}{\theta \Delta t} + \alpha G \mathbf{V}^{n+\theta} + (1 - \alpha) G \mathbf{V}^n &= 0. \end{aligned}$$

In second stage, solve the pair $(\mathbf{U}^{n+1-\theta}, \mathbf{V}^{n+1-\theta})$ as:

$$\begin{aligned} \mathbf{M} \frac{\mathbf{U}^{n+1-\theta} - \mathbf{U}^{n+\theta}}{(1 - 2\theta) \Delta t} + (1 - \alpha) K \mathbf{U}^{n+1-\theta} + \alpha K \mathbf{U}^{n+\theta} \\ - (1 - \alpha) \hat{F}(\mathbf{U}^{n+1-\theta}) - \alpha \hat{F}(\mathbf{U}^{n+\theta}) &= 0, \\ \mathbf{N} \frac{\mathbf{V}^{n+1-\theta} - \mathbf{V}^{n+\theta}}{(1 - 2\theta) \Delta t} - \mathbf{P} \frac{\mathbf{U}^{n+1-\theta} - \mathbf{U}^{n+\theta}}{(1 - 2\theta) \Delta t} + (1 - \alpha) G \mathbf{V}^{n+1-\theta} + \alpha G \mathbf{V}^{n+\theta} &= 0. \end{aligned}$$

Finally in third stage, solve the pair $(\mathbf{U}^{n+1}, \mathbf{V}^{n+1})$ as:

$$\begin{aligned} \mathbf{M} \frac{\mathbf{U}^{n+1} - \mathbf{U}^{n+1-\theta}}{\theta \Delta t} + \alpha K \mathbf{U}^{n+1} + (1 - \alpha) K \mathbf{U}^{n+1-\theta} - \alpha \hat{F}(\mathbf{U}^{n+1}) \\ - (1 - \alpha) \hat{F}(\mathbf{U}^{n+1-\theta}) &= 0, \\ \mathbf{N} \frac{\mathbf{V}^{n+1} - \mathbf{V}^{n+1-\theta}}{\theta \Delta t} - \mathbf{P} \frac{\mathbf{U}^{n+1} - \mathbf{U}^{n+1-\theta}}{\theta \Delta t} + \alpha G \mathbf{V}^{n+1} + (1 - \alpha) G \mathbf{V}^{n+1-\theta} &= 0. \end{aligned}$$

In our computation, we fixed $\theta = 1 - \frac{1}{2}\sqrt{2}$ and $\alpha = 2\theta$. At each time level, the linear and nonlinear terms are solved using BiConjugate Gradient (BiCG) method (Saad, 2003) and Newton’s method (Quarteroni, Sacco, & Saleri, 2008), respectively.

The adaptive time-stepping algorithm is given as follows:

Algorithm 1 Adaptive time-stepping process

```

Given:  $\mathbf{W}_n = \begin{bmatrix} c_n \\ T_n \end{bmatrix}$ , Tol= $10^{-6}$ ,  $\Delta t_{start} = 10^{-4}$ ,  $\Delta t_{max} = 10^{-2}$ , End Time = 0.4
while Time < End Time do
  Compute  $\mathbf{W}_{n+1}$  using  $\Delta t$ 
  Calculate  $e_{n+1} = \|\mathbf{W}_{n+1} - \mathbf{W}_n\|$ 
  if  $e_{n+1} > \text{Tol}$  then
     $\Delta t_n = \Delta t_n / 2$ 
    Recompute  $\mathbf{W}_{n+1}$ ,
  else
    Update the time step.
    If  $\Delta t_n < \Delta t_{max}$ 
       $\Delta t = \min(\sigma \Delta t_n, \Delta t_{max})$ ; where  $\sigma$  is adaptive factor.
    end if
  end while

```

Table 2. Comparison of different time discretization schemes for $\sigma = 1.2$.

$\sigma = 1.2$	TIME STEPS	MAX L-IT	MAX NL-IT	CPU TIME	LS TIME
DIFST	61	1174	471	2254	85.99
DIRK3	Fails after 27 time steps with $\Delta t > 9.5396 \times 10^{-3}$				
DIRK2	Fails after 25 time steps with $\Delta t > 1.0 \times 10^{-2}$				

Table 3. Comparison of different time discretization schemes for $\sigma = 2.0$.

$\sigma = 2.0$	TIME STEPS	MAX L-IT	MAX NL-IT	CPU TIME	LS TIME
DIFST	46	1116	403	1850.1	77.555
DIRK3	Fails after 6 time steps with $\Delta t > 1.0 \times 10^{-2}$				
DIRK2	Fails after 9 steps with $\Delta t > 4.6 \times 10^{-3}$				

4. Numerical results and discussion

In this section, we assess the time-step stability of the proposed DIFST scheme. Our goal is to find the maximum time-step size at which a given dendritic crystal growth model is solvable. We also provide efficiency and robustness of the DIFST scheme in comparison with DIRK2 and DIRK3 schemes (Alexander, 1977) using different values of adaptivity factor in Algorithm 1. Table 1 shows that both DIFST and DIRK3 schemes work for small adaptive factor $\sigma = 1.1$, but DIRK2 scheme diverges after 46 iterations. Tables 2 and 3 show that for $\sigma = 1.2$ and 2.0 both DIRK2 and DIRK3 schemes diverge after few iteration, while DIFST scheme works well resulting in the reduction in simulation time. We have calculated the computational cost in term of maximum linear iterations (MAX L-IT), maximum non-linear iterations (MAX NL-IT), central processing unit time (CPU TIME) and linear solver time (LS TIME).

In two-phase flow problems like dendritic crystal growth, the coupling of time-dependent interface equation plays a crucial role. However, it requires large computational cost due to small time-step stability constraint. Even if the interface is nearly stationary, large time-step will generate spurious oscillations

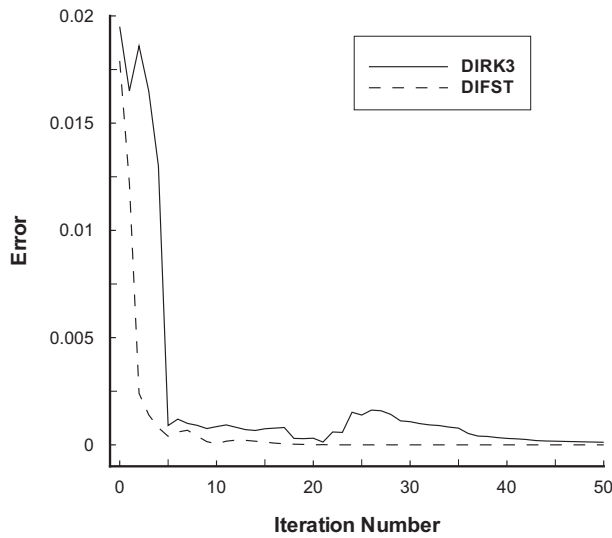


Figure 2. Numerical errors for DIRK3 and DIFST schemes.

in the solution. To handle this issue, we proposed a technique given in Algorithm 1 that has relaxed the time-step restriction. Figure 2 shows the comparison of error between DIFST and DIRK3 schemes for $\sigma = 1.1$, proving that the DIFST scheme is more stable.

The computed results for dendritic growth c and temperature T at different time levels using Algorithm 1 are given in Figure 3, which are comparable with results using the finite difference method of T. Biben Biben (2005) as shown in Figure 4. From qualitative comparison of Figures 3–4, we observed faster growth, better resolution with pattern formation using the proposed method. The effect of some important parameters on the shape and size of dendrite is given in the next Section 5.

5. Parametric study

For fixed values of $\beta = .9$, $\eta = 1.0$, anisotropy $a_0 = 6.0$, orientation of anisotropy $\theta_0 = 1.57$, and $\Delta x = \Delta y = .03$ over the mesh domain $[0, 300] \times [0, 300]$, the effects of latent heat k , melting temperature T_m , relaxation time τ , interfacial width ϵ_0 and modulation of interfacial width μ are investigated at $t = .2$.

5.1. Effect of latent heat

The latent heat ' k ' is the main parameter which triggers the solidification process and therefore has great importance in solving dendritic crystal growth problems. Figure 5 shows that large values of ' k ' account for the evacuation of more heat from the interfacial region. Therefore, the growth of dendrite is directly

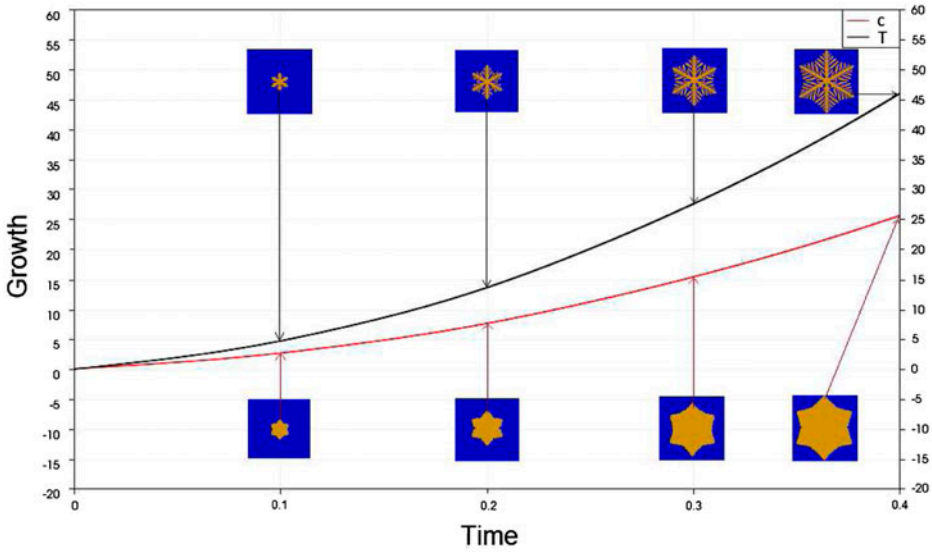


Figure 3. Calculation of c and T at $t = .1, t = .2, t = .3,$ and $t = .4$ using present scheme.

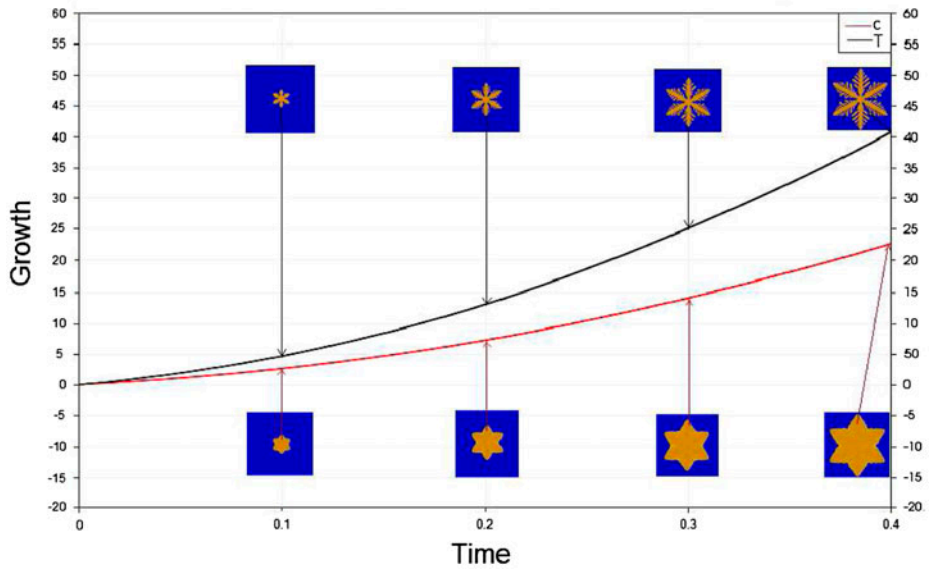


Figure 4. Calculation of c and T at $t = .1, t = .2, t = .3,$ and $t = .4$ using Euler scheme Biben (2005).

proportional to the value of ' k '. Figure 5 shows the dendritic growth for different latent heats $k = .5, 1.0$ and 1.8 , which clearly demonstrates that the shape of dendrite is directly effected by the latent heat. As latent heat increases from $.5$ to 1.8 , the tip radius and tip velocity of side branches also increases. Small value of ' k ' can therefore limit the growth of side branches.



Figure 5. Effect of latent heat $k = .5, 1.0,$ and 1.8 (left to right) on dendrite.



Figure 6. Effect of melting temperature $T_m = .9, 1.0,$ and 1.2 (left to right) on dendrite.

5.2. Effect of melting temperature

In this subsection, simulation results for $T_m = .9, 1.0$ and 1.2 at time $t = .2$ are given in Figure 6 to show its effect on the growth, size and shape of dendrite. It is observed that increasing the value of ' T_m ' accelerates growth process. It can also be seen from Figure 6 that increasing ' T_m ' increases the tip velocity, while tip radius of side branches has an inverse effect. By increasing ' T_m ', the growth rate decreases i.e. the dendrite have larger radii while side branches grow with less speed. It is to be noted that increasing ' T_m ' beyond the melting point will melt the structure.

5.3. Effect of relaxation time

The relaxation time measurement can provide many insights into molecular and atomic structures along with rates and mechanisms of chemical reactions. In Figure 7, the relaxation time effect on dendrite for $\tau = .0002, .0003$ and $.0004$ is given at time $t = .2$. It shows that for $\tau = .0002$, the dendrite grow faster than other values which shows that for small values of ' τ ', the atoms need less time to attain their equilibrium state, while for large values of ' τ ' it reaches their equilibrium state lately. Indirect effect of ' τ ' on the tip velocity and tip radius of side branches is also observed. From Figure 7, we notice that increasing from $\tau = .0002$ to $.0004$, the tip radius and tip velocity of side branches decrease.



Figure 7. Effect of relaxation time $\tau = .0002, .0003, \text{ and } .0004$ (left to right) on dendrite.



Figure 8. Effect of interfacial width $\epsilon_0 = .009, .01, \text{ and } .011$ (left to right) on dendrite.

5.4. Effect of interfacial width

We have computed the results for different values of interfacial width $\epsilon_0 = .009, .01$ and $.011$ as shown in Figure 8, respectively, at time $t = .2$. The growth process is faster for larger values of ϵ_0 . It is also observed that modulation of interfacial width μ_0 does not effect the tip radius and velocity of growing branches.

6. Conclusions

In this work, we proposed the efficient time adaptive algorithm for the numerical simulation of nonlinear system of PDEs for dendritic crystal growth. For numerical computation, DUNE plate-form is used specially DUNE-PDELab. The space discretisation is done by Q_1 conforming FEM while DIFST scheme is used for time discretisation. The BICG method and Newton's method are used to solve the resulting Linear and non-linear system of equations, respectively. The DIFST scheme is compared with traditional DIRK scheme of order 2 and 3 for small and large adaptive factors. Efficiency and robustness of proposed scheme is observed for numerical simulation of dendritic crystal growth. Effects of different parameters on the shape and size of dendritic crystal are studied. Future work may include the development of adaptive grid strategies using parallel computing to solve more realistic three-dimensional problems.

Disclosure statement

No potential conflict of interest was reported by the authors.

Funding

This work was carried out while M. Sabir was visiting IWR, University of Heidelberg Germany. The visit was financially supported by EMMAAsia 2012.

ORCID

Abdullah Shah  <http://orcid.org/0000-0002-0337-1216>

References

- Alexander, R. (1977). Diagonally implicit Runge-Kutta methods for stiff O.D.E's. *SIAM Journal on Numerical Analysis*, 14, 1006–1021.
- Bastian, P., Blatt, M., Dedner, A., Engwer, C., Klöforn, R., Kornhuber, R., ... Sander, O. (2008). A generic grid interface for parallel and adaptive scientific computing. Part II: Implementation and tests in DUNE. *Computing*, 82, 121–138.
- Bastian, P., Blatt, M., Dedner, A., Engwer, C., Klöforn, R., Ohlberger, M., & Sander, O. (2008). A generic grid interface for parallel and adaptive scientific computing. Part I: Abstract framework. *Computing*, 82, 103–119.
- Bastian, P., Blatt, M., Engwer, C., Dedner, A., Klöforn, R., Kuttanikkad, S. P., & Sander, O. (2006). The distributed and unified numerics environment. In *Proceedings 19th Symposium Simulation Technical*, Hanover.
- Bastian, P., & Helmig, R. (1999). Efficient fully-coupled solution techniques for two-phase flow in porous media: Parallel multigrid solution and large scale computations. *Advances in Water Resources*, 23, 199–216.
- Bastian, P., & Rivière, B. (2004). *Discontinuous galerkin methods for two-phase flow in porous media*, Technical Report. IWR: University of Heidelberg. 24.
- Biben, T. (2005). Phase-field models for free-boundary problems. *The European Journal of Physics*, 26, 147–55.
- Blatt, M., & Bastian, P. (2007). The iterative solver semplate library. *Applications Parallel Computing*, 4699, 666–675.
- Blatt, M., & Bastian, P. (2008). On the generic parallelisation of iterative solvers for the finite element method. *Physica D: Nonlinear Phenomena*, 4, 56–69.
- Boettinger, W. J., Coriell, S. R., Greer, A. L., Karma, A., Kurz, W., Rappaz, M., & Trivedi, R. (2000). Solidification microstructures: Recent developments, future directions. *Acta Metallurgica*, 48, 43–70.
- Bollada, P., Jimack, P., & Mullis, A. (2012). A new approach to multi-phase formulation for the solidification of alloys. *Physica D: Nonlinear Phenomena*, 241, 816–829.
- Collins, J., & Levine, H. (1985). Diffuse interface model of diffusion-limited crystal growth. *Physica D: Nonlinear Phenomena*, 31, 6119–6122.
- Copley, S. M., Todd, J. A., Yankova, M., & Yankov, E. Y. (1996). Solidification of Agcu alloys at high growth rates produced by continuous laser melt quenching. *Laser Processing*, 307, 92–119.
- Dedner, A., Klöforn, R., Nolte, M., & Ohlberger, M. (2010). A generic interface for parallel and adaptive discretization schemes: Abstraction principles and the Dune-Fem module. *Philosophical Transactions of the Royal Society*, 90, 165–196.

- Fix, G. J. (1983). Free boundary problems: Theory and applications. *Pitman, Boston*, 2, 580–589.
- Glowski, R. (2003). Finite element methods for incompressible viscous flow. *Handbook Numerical Analysis*, 9, 3–1171.
- Goodyer, C., Jimack, K., Mullis, A., Dong, H., & Xie, Y. (2012). On the fully implicit solution of a phase-field model for binary alloy solidification in three dimensions. *Advances in Applied Mathematics and Mechanics*, 4, 665–684.
- Haxhimali, T., Karma, A., Gonzales, F., & Rappaz, M. (2006). Orientation of selection in dendritic evolution. *Nature Materials*, 5, 2016–2024.
- Hughes, T. J. R. (2008). The finite element method: Linear static and dynamic finite element analysis. *Computer-Aided Civil Infrastructure Engineering*, 4, 245–246.
- Kobayashi, R. (2006). Modeling and numerical simulations of dendritic crystal growth. *Journal of Computational Physics*, 218, 770–793.
- Madzvamuse, A. (2006). Time-stepping schemes for moving grid finite elements applied to reaction diffusion systems on fixed and growing domains. *Journal of Computer Physics*, 214, 239–263.
- McFadden, G. B., Wheeler, A. A., Braun, R. J., Coriell, S. R., & Sekerkan, R. F. (1993). Phase-field models for anisotropic interfaces. *Physical Review E*, 48, 2016–2024.
- Mullis, A., Bollada, P., & Jimack, P. (2014). Towards a 3-dimensional phase-field model of non-isothermal alloy solidification. *Materials Science Forum*, 783, 2166–2171.
- Mullis, A., Goodyer, C., & Jimack, P. (2012). Towards a 3-dimensional phase-field model of dendritic solidification with physically realistic interface width. *Transactions of the Indian Institute of Metals*, 65, 617–621.
- Nishinaga, T., & Rudolph, P. (2014). Handbook of crystal growth. *Condensed Matter Physics*, 2, 1075–1080.
- Osher, S., & Sethian, J. A. (1988). Fronts propagating with curvature-dependent speed: Algorithm based on one Hamilton–Jacobi formulations. *Journal of Computational Physics*, 79, 12–49.
- Quarteroni, A., Sacco, R., & Saleri, F. (2008). Texts in applied mathematics. *Numerical Mathematics*, 37, 1–4.
- Ruuth, S. J. (1995). Implicit-explicit methods for reaction-diffusion problems in pattern formation. *Journal of Mathematical Biology*, 34, 148–176.
- Saad, Y. (2003). Iterative methods for sparse linear systems. *SAIM*, 2, 217–244.
- Shah, A., Haider, A., & Shah, S. K. (2014). Numerical simulation of two-dimensional dendritic growth using phase-field model. *World Journal of Mechanics*, 4, 128–136.
- Thomee, V. (2006). Galerkin finite element methods for parabolic problems. *Springer Series in Computer Mathematics*, 25, 2016–2024.
- Wang, S. L., & Sekerka, R. F. (1993). Thermodynamically-consistent phase-field models for solidification. *Physica D: Nonlinear Phenomena*, 69, 189–200.
- Wheeler, A. A., Murray, B. T., & Schaefer, R. J. (1993). Computation of dendrites using a phase field model. *Physica D: Nonlinear Phenomena*, 66, 243–262.